ARTICLE

Electronic Supporting Information (ESI)

Improving high-voltage high-rate performance of P2 layered oxide cathode by dual-ion doping strategy for sodium-ion batteries

Huan Xu[a], Chengde Xie[a], Huige Chen[b], Tianyi Song[a], Yuanqi Lan[a,c], Nanzhong Wu[a, c], Xiaolong Zhou[a], Pinit Kidkhunthod[d], Lei Kang[b], Xiaoqi Han[a], Wenjiao Yao[a, c,e*], Yongbing Tang[a, c *]

[a.] *Advanced Energy Storage Technology Research Center, Shenzhen Key Laboratory of Energy Materials for Carbon Neutrality, Shenzhen Institute of Advanced Technology, Chinese Academy of Sciences, Shenzhen, 518055, China. Email: wj.yao@siat.ac.cn, tangyb@siat.ac.cn*
[b.] *Functional Crystals Lab, Technical Institute of Physics and Chemistry, Chinese Academy of Sciences, Beijing 100190, China*
[c.] *Shenzhen College of Advanced Technology, University of Chinese Academy of Sciences, Beijing 100049, China*
[d.] *Synchrotron Light Research Institute, Nakhon Ratchasima 30000, Thailand.*
[e.] *Shenzhen Key Laboratory of Energy Materials for Carbon Neutrality, Shenzhen 518055, China*

Experiment Section:

Material synthesis:

All samples in this study were synthesized by the high-temperature solid-state method. A detailed preparation process is included in the following. Pristine P2-$Na_{2/3}Ni_{1/3}Mn_{2/3}O_2$ samples were synthesized by mixing stoichiometrically Na_2CO_3 (AR, Sigma-Aldrich), NiO (AR, Sigma-Aldrich), and MnO_2 (AR, Sigma-Aldrich) in the mortar with moderate amounts of ethanol, ball-milling for 300 min at a rate of 350 r/min. The mixture was then pressed into pellets of 10-mm diameter and sintered in a Muffle furnace at 900℃ for 10 h. Final samples were obtained after grinding. The doping samples were acquired by the same steps but adjusting reactants stoichiometrically, with additional TiO_2 (AR, Sigma-Aldrich), and/or NaF (AR, Sigma-Aldrich) in the original ingredients.

Material characterization:

Powder XRD patterns were collected by a Rigaku diffractometer (MiniFlex600) with Cu Kα radiation (λ = 0.154056 nm). Scans were taken from 10-90° with a 2θ step of 0.02°. Rietveld method was used to refine the data sets using the GSAS package incorporated with the EXPGUI interface[1]. Parameters, such as scale factor, background, lattice parameters, and zero point were refined until convergence. In-situ XRD patterns were recorded on a SmartLab operated at 40 kV and 15 mA using Cu Kα radiation in the 2θ range 5–90° equipped with a battery test system (NEWARE CT-4008). Scanning electron microscope (SEM) measurements and energy dispersion X-ray spectra (EDS) element mapping of the samples were carried out on ZEISS SUPRA 55 equipped with an EDS analyzer. Transmission electron microscope (TEM) was conducted by a JEOL JEM-F200 field emission TEM equipped with an Oxford Instruments EDS analyzer. The chemical composition of the obtained materials was performed by inductively coupled plasma-atomic emission spectroscopy (ICP-AES, PE optima 6000). X-ray photoelectron spectroscopy (XPS) measurements were performed using a Thermo Escalab 250Xi X-ray photoelectron spectrometer (Thermo, USA). Raman spectra were carried out using HORIBA, XploRA PLUS detector in the backscattering mode at the 400–2000 cm^{-1} frequency range. The wave number resolution and probe aperture are 1 cm^{-1} and about 10 μm, respectively. Synchrotron X-ray absorption spectroscopies (XAS) experiments were conducted at the Ni K-edge (8333 eV), Mn K-edge (6539 eV) and Ti K-edge (4966 eV) on SUT-NANOTEC-SLRI XAS beamline (BL5.2), Synchrotron Light Research Institute (SLRI, public organization), Thailand. The beamline photo source covers an energy range of 1810 eV to 13000 eV, with an energy resolution of 2×10^{-4}. Data were acquired in fluorescence mode using Si drift detector. Spectra were obtained at room temperature. XAS data were processed and analyzed using the Demeter software package[2].

First-principles calculation:

The present first-principles calculations were performed by the plane-wave ultrasoft pseudopotential method using CASTEP based on the density functional theory (DFT) [3–5]. The simulation models for this study were the P2-$Na_{16}Ni_4Mn_8O_{24}$ and P2-$Na_{16}Ni_4Mn_5Ti_3O_{23}F$ structures. The exchange and correlation energy were treated using the local density approximation (LDA, CA-PZ) functional. A cutoff energy of 280 eV was selected for the plane-wave basis set. The Monkhorst-Pack k-point density with 3×2×1 was used in the Brillouin zone [6]. Spin-polarization was employed throughout all calculations. The convergence criteria of energy, force, stress, and displacement were respectively set as 5.0×10^{-5} eV per atom, 0.1 eV $Å^{-1}$, 0.2 GPa, and 5.0×10^{-3} Å, respectively. The complete linear synchronous transit/quadratic synchronous transit (LST/QST) method was used to calculate the Na diffusion energy barriers in P2-NNM and the P2-NNMT0.1-F0.05 composites [7].

Electrochemical measurement:

Cathode electrodes were prepared by casting the slurry (80 wt.% active material, 10 wt.% super P, 10 wt.% polyvinylidene fluoride (PVDF, AR, Sigma-Aldrich) and an appropriate amount of N-methyl-2-pyrrolidone (NMP, Sigma-Aldrich) onto aluminum foil and dried in a vacuum at 80℃ for overnight. The loading mass of the active material is about 2 mg cm^{-2}. The hard carbon anode was prepared in a similar way but on a copper foil.

The CR2032 coin cells were assembled in a glove box filled with Ar (H_2O and O_2 < 0.1 ppm). Pure Na foil was used as a counter electrode and a glass fiber (Whatman GF/A) was used as the separator. The electrolyte was 1 M $NaClO_4$ (AR, Sigma-Aldrich) in propylene carbonate (PC, AR, Sigma-Aldrich) with 5 vol% fluoroethylene carbonate (FEC, AR, Sigma-Aldrich). Galvanostatic charge-discharge (GCD) and rate performance tests were carried out on a test system (NEWARE CT-4008). The current densities and capacities of electrodes were calculated based on the weight of active materials (1C = 173 mA g^{-1}). Cyclic voltammetry (CV) and electrochemical impedance spectroscopy (EIS) tests were measured on an electrochemical workstation (AUTOLAB M204). CV tests were performed in the voltage range of 1.5 V–4.3 V and 2.3 V–4.3 V vs. Na^+/Na at the scan rates from 0.1 to 1.0 mV s^{-1}. Full cells were assembled in the same way as half-coin cells but changed the Na foil to pre-sodiated hard carbon anode, and the N/P is about 1.2. The specific capacity and energy density of the full cell are calculated based on the active mass of the cathode material.

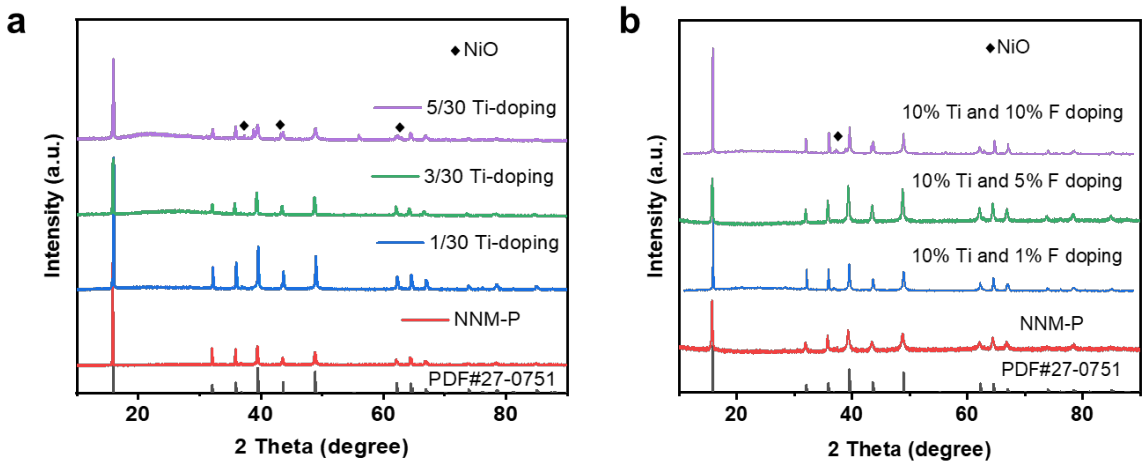

Figure S1 XRD comparison of different Ti or/and F-substituted $Na_{2/3}Ni_{1/3}Mn_{2/3-x}Ti_xO_{2-y}F_y$ (x = 0, 1/30, 3/30, 5/30, y = 0, 0.01, 0.05, 0.1) cathode materials.

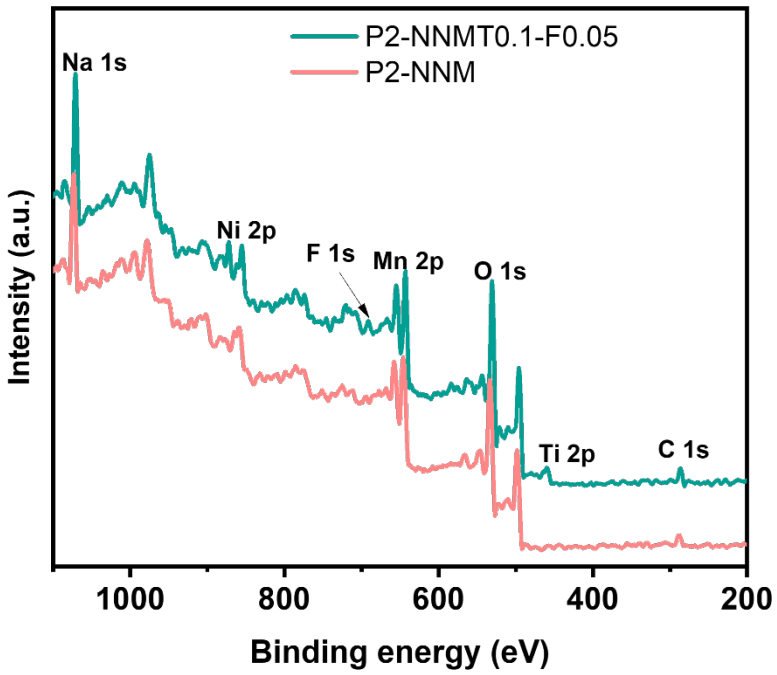

Figure S2. XPS overall map of pristine and Ti and F doping P2-NNM samples.

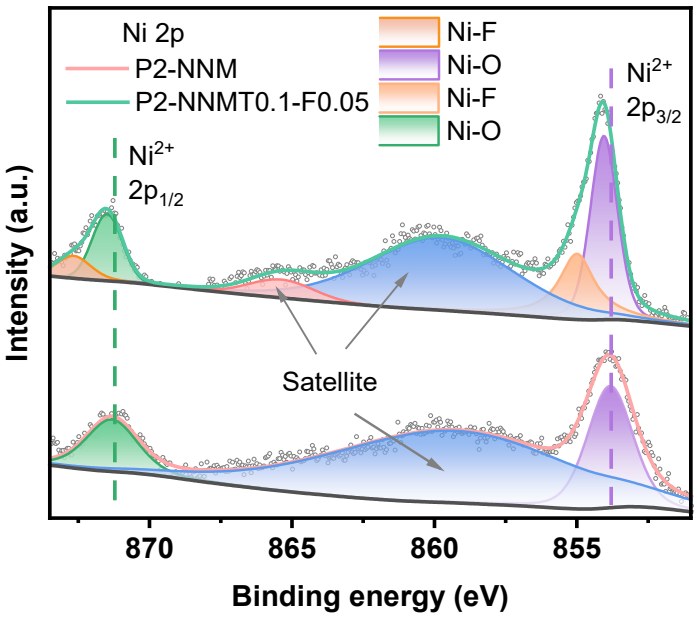

Figure S3. Ni 2p fitting results of pristine and Ti and F doping P2-NNM samples.

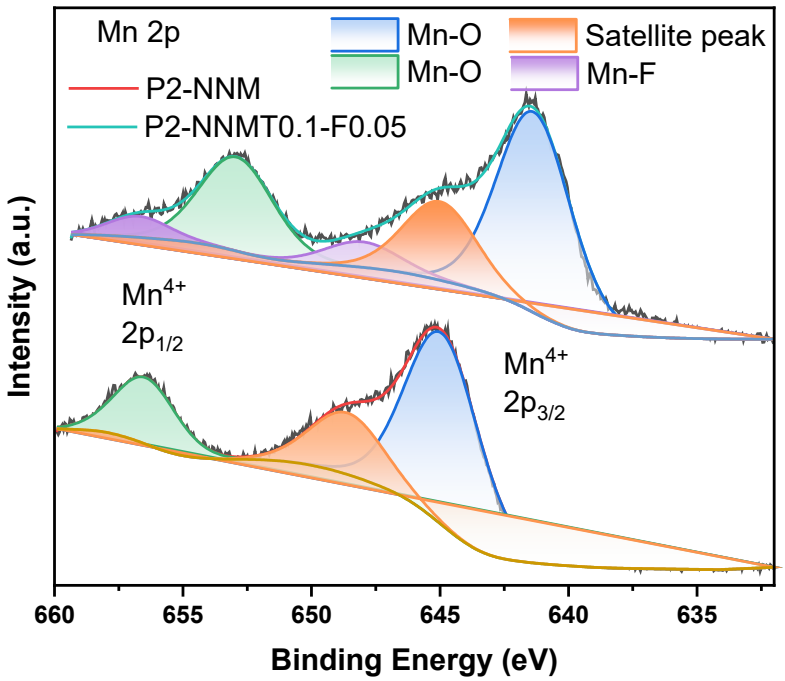

Figure S4. Mn 2p fitting results of pristine and Ti and F doping P2-NNM samples.

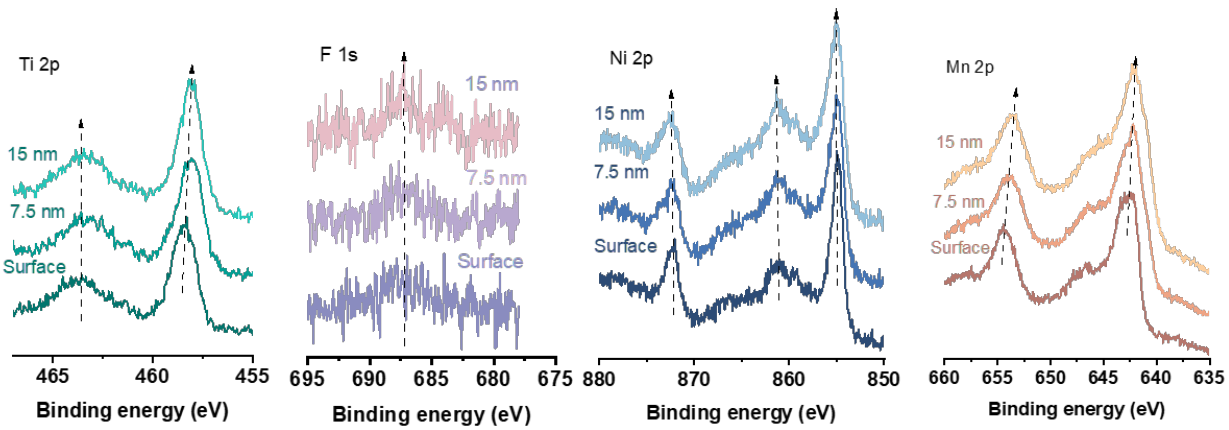

Figure S5. XPS with different etching depth of Ti 2p, F 1s, Ni 2p, Mn 2p Ti and F doping P2-NNM sample.

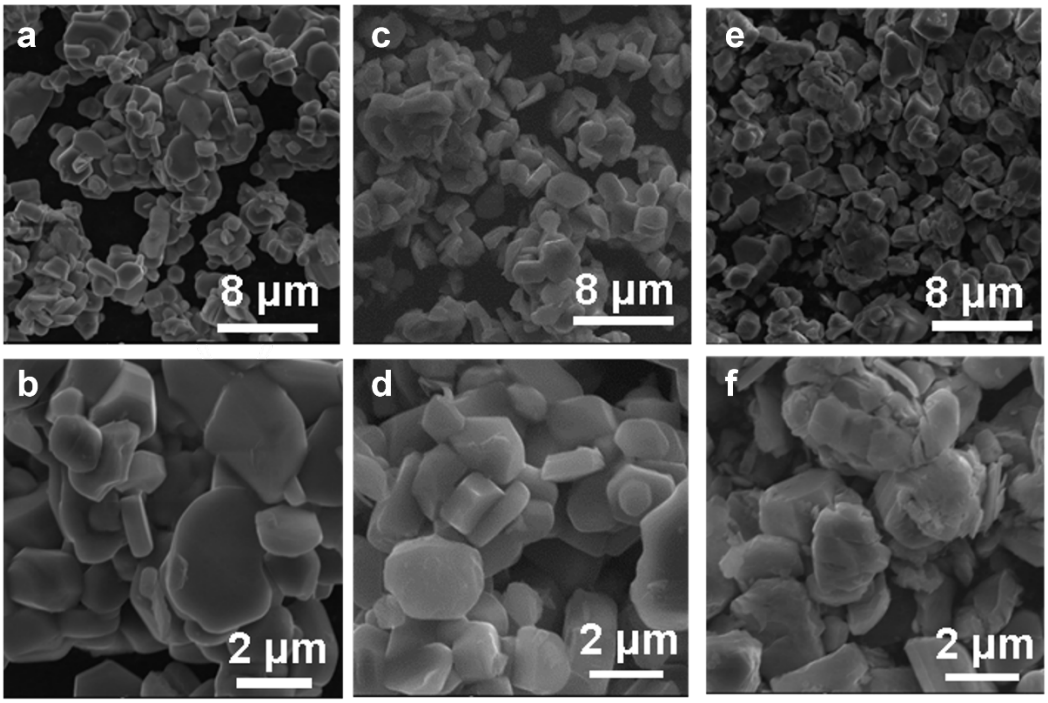

Figure S6. SEM images of different F doping samples. (a-b) 1% F. (c-d) 5% F. (e-f) 10% F.

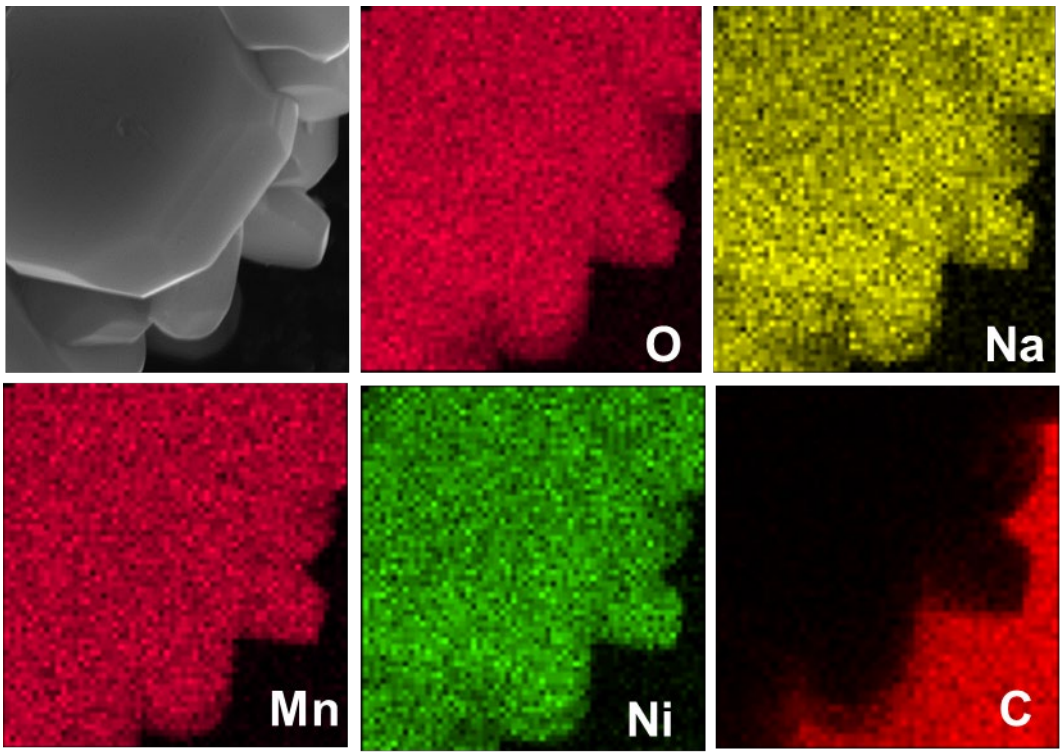

Figure S7. EDS mapping of P2-NNM sample.

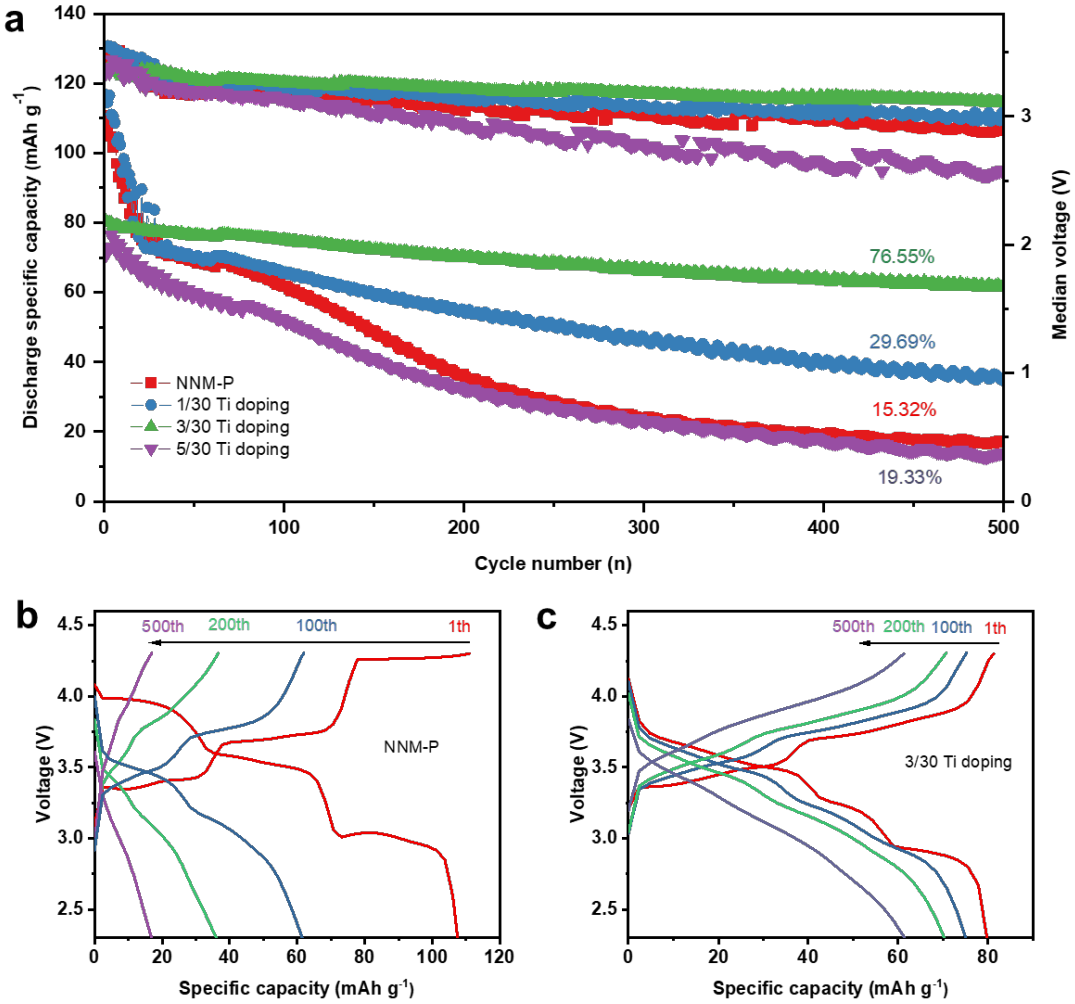

Figure S8. (a) Long cycle performance of different amount of Ti doping at 5C. (b) Charge-discharge curve for pristine NNM. (c) Charge-discharge curve for NNM with 3/30 Ti doping.

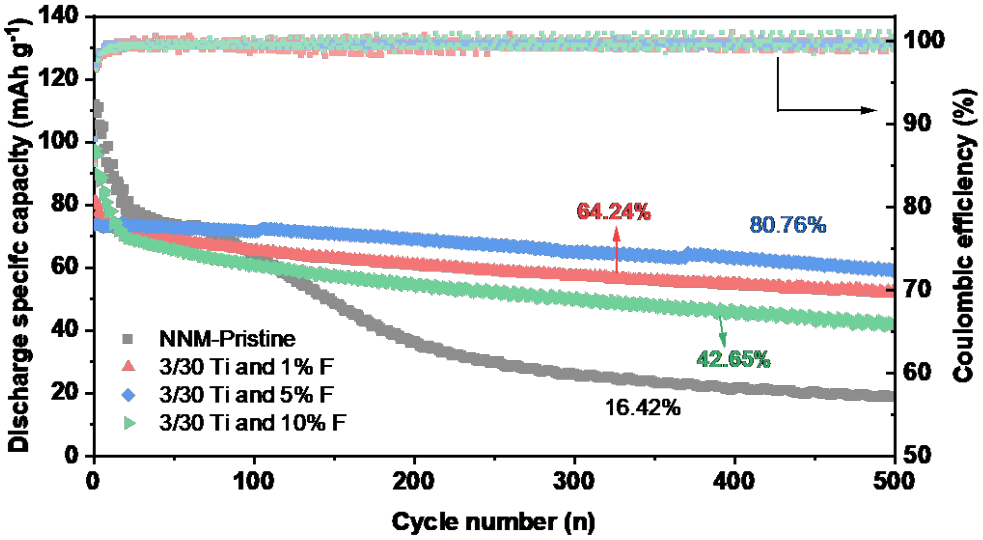

Figure S9. Cycle performance of NNM pristine and 10% Ti and different F doping (1%, 5%, 10%) samples.

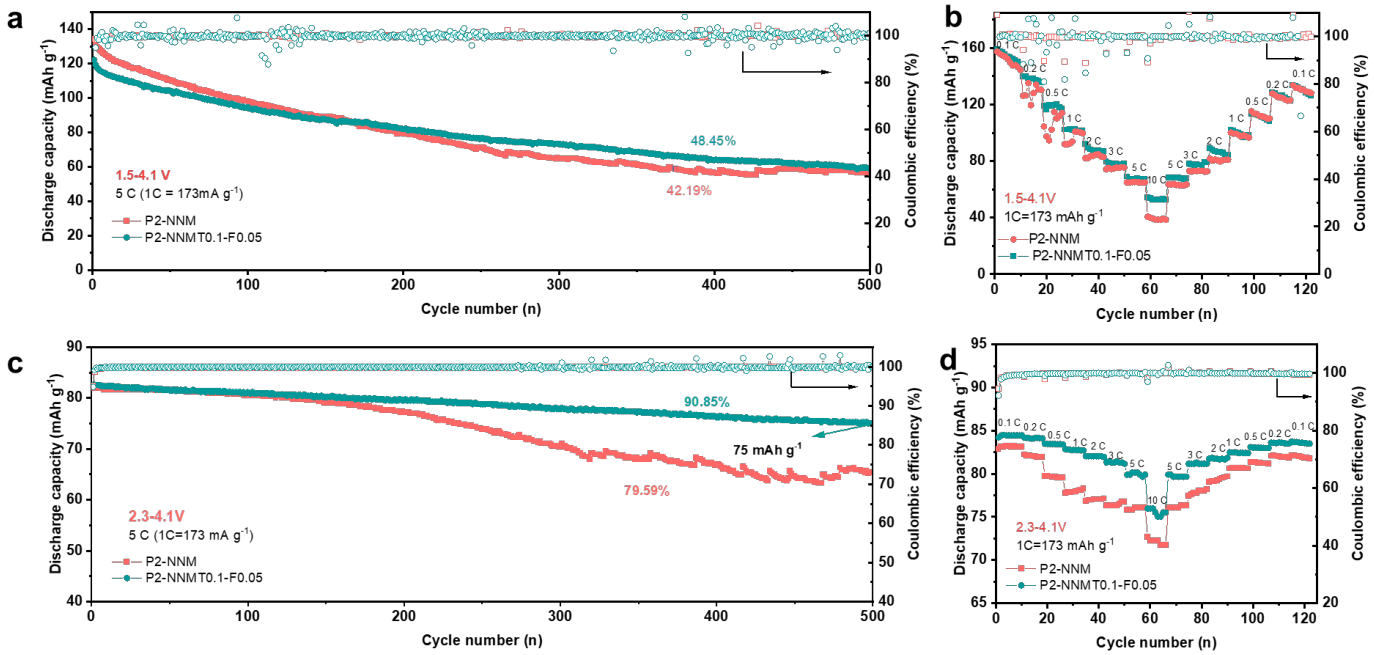

Figure S10. (a) Cycle performance at 1.5-4.1 V. (b) Rate performance at 1.5-4.1 V. (c) Cycle performance at 2.3-4.1 V of pristine NNM and 10% Ti and 5% F co-doping samples.

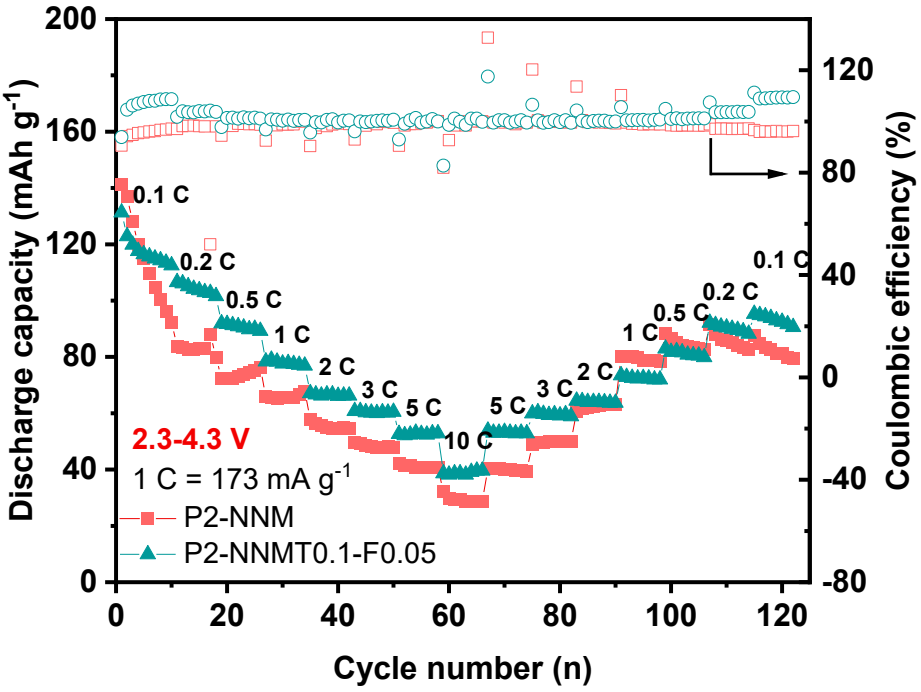

Figure S11. Rate performance at 2.3-4.3 V.

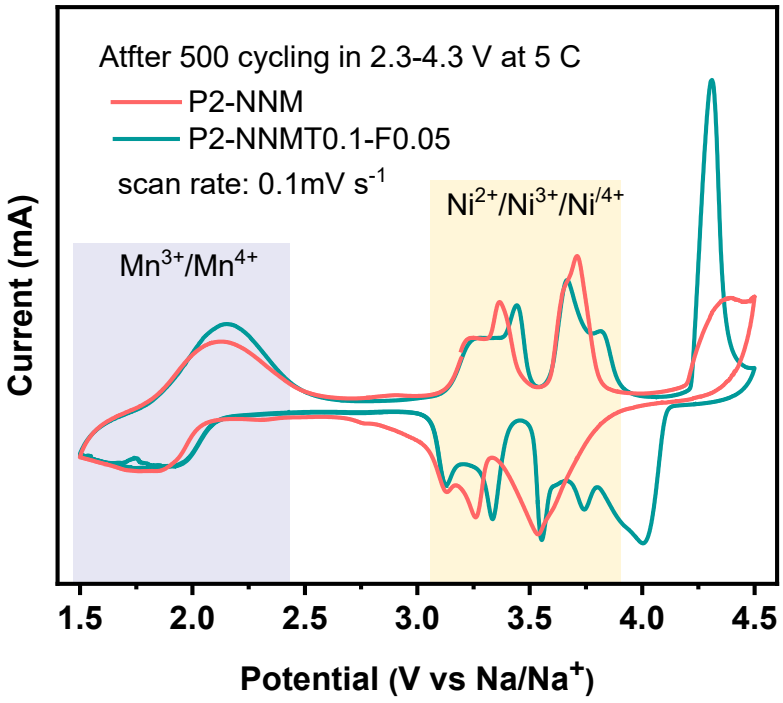

Figure S12. CV curves of NNM pristine and Ti and F co-doping samples at 1.5-4.5 V.

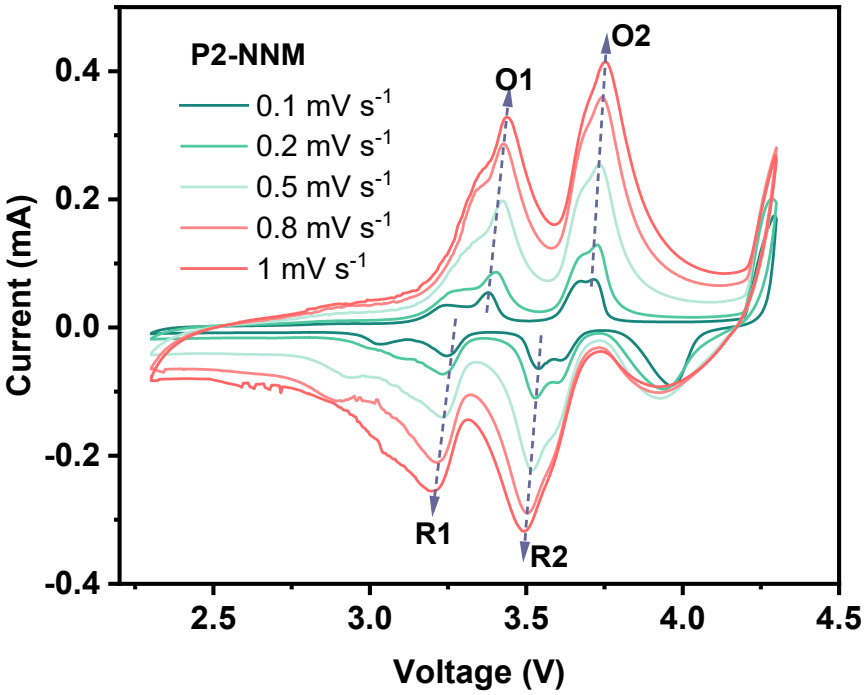

Figure S13. CV curves of P2-NNM at different scan rates from 0.1 to 1.0 mV s^{-1}.

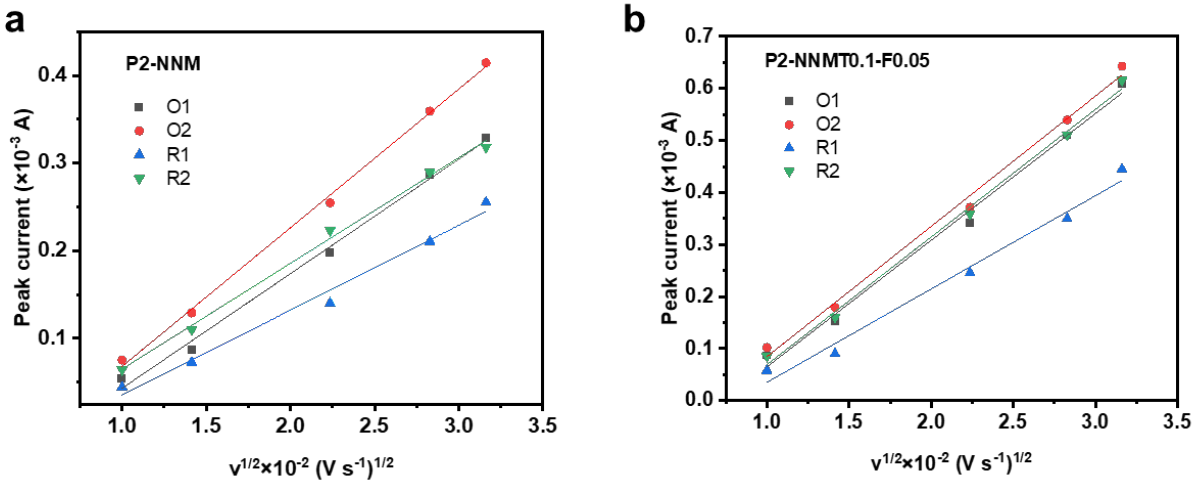

Figure S14. the corresponding fitting curves between peak currents (ip) and the square root of scan rates ($v^{1/2}$) of (a) P2-NNM. (b) P2-NNMT0.5-F0.05.

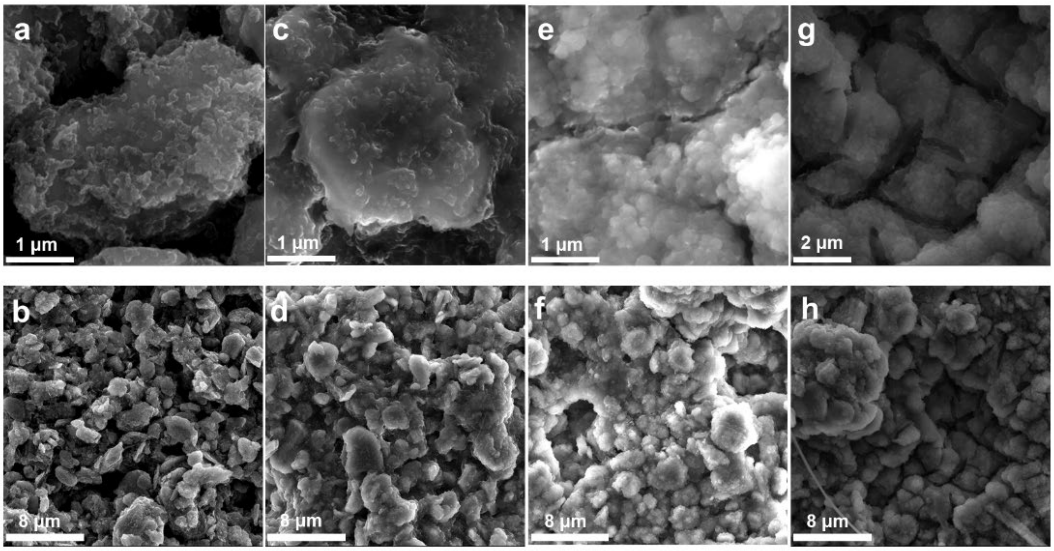

Figure S15. SEM images of NNM-Pristine samples before and after cycling at 5C in different voltage ranges. (a-b) before cycling, (c-d) 2.3-4.1 V, (e-f) 1.5-4.1 V, (g-h) 2.3-4.3 V.

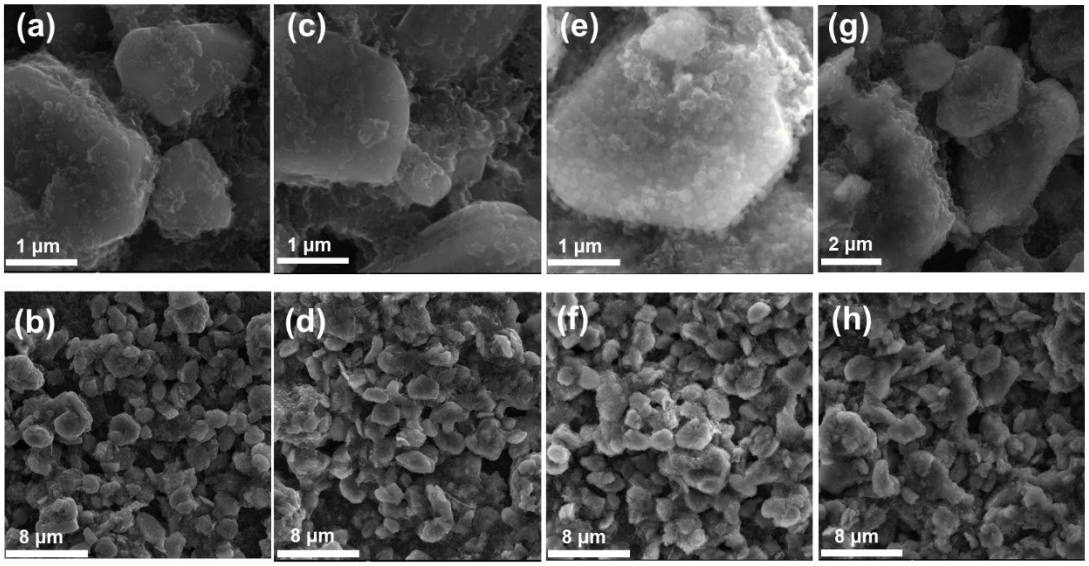

Figure S16. SEM images of 10% Ti and 5% F co-doping samples before and after cycling at 5C in different voltage ranges. (a-b) before cycling. (c-d) 2.3-4.1 V. (e-f) 1.5-4.1 V. (g-h) 2.3-4.3 V.

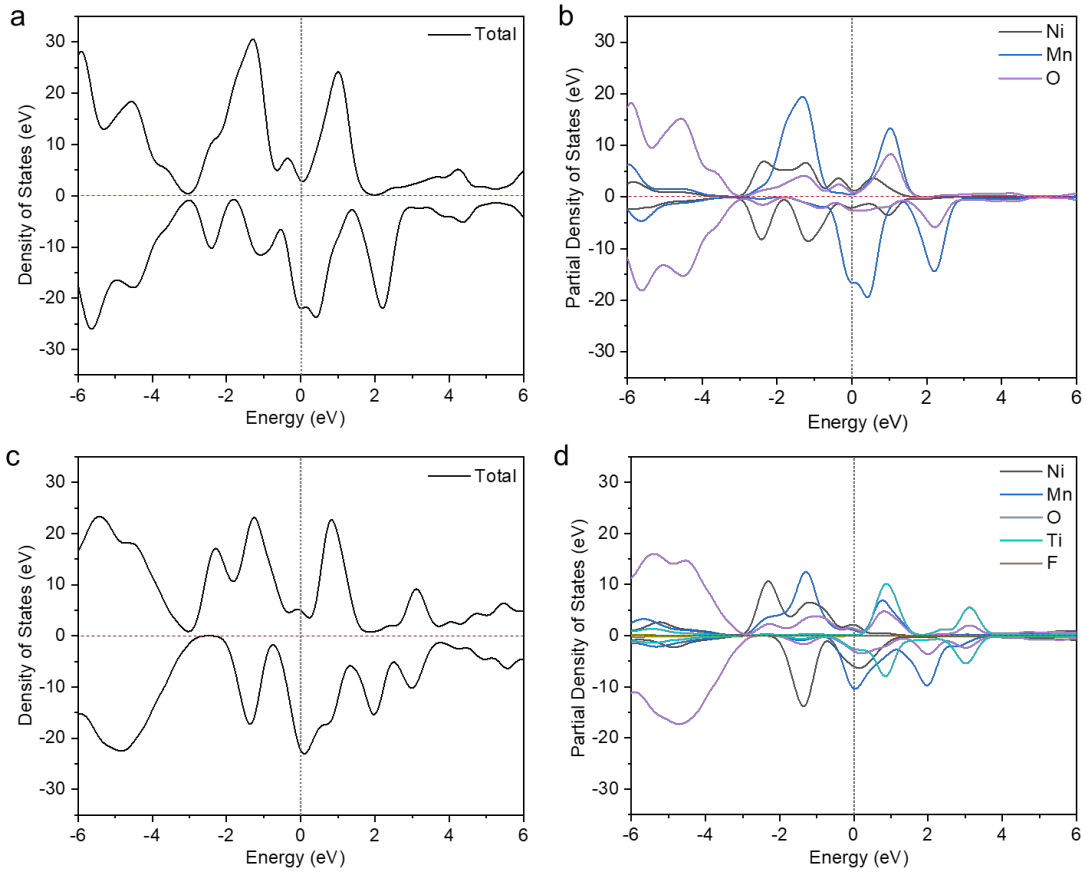

Figure S17. (a) The total density of state of pristine sample. (b) Partial density of states (pDOS) of O 2p, Mn 3d, and Ni 3d orbitals of pristine sample. (c) The total density of state of Ti and F doping sample. (d) pDOS of O 2p, Mn 3d, and Ni 3d orbitals of Ti and F doping sample.

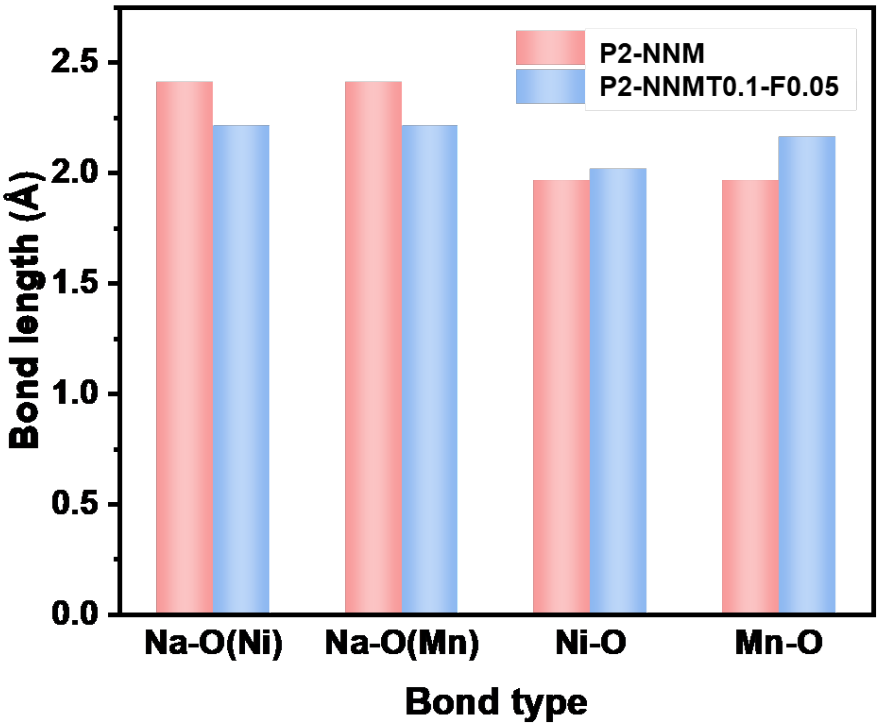

Figure S18. Comparison of the average bond lengths in the pristine P2-NNM and P2-NNMT0.1-F0.05.

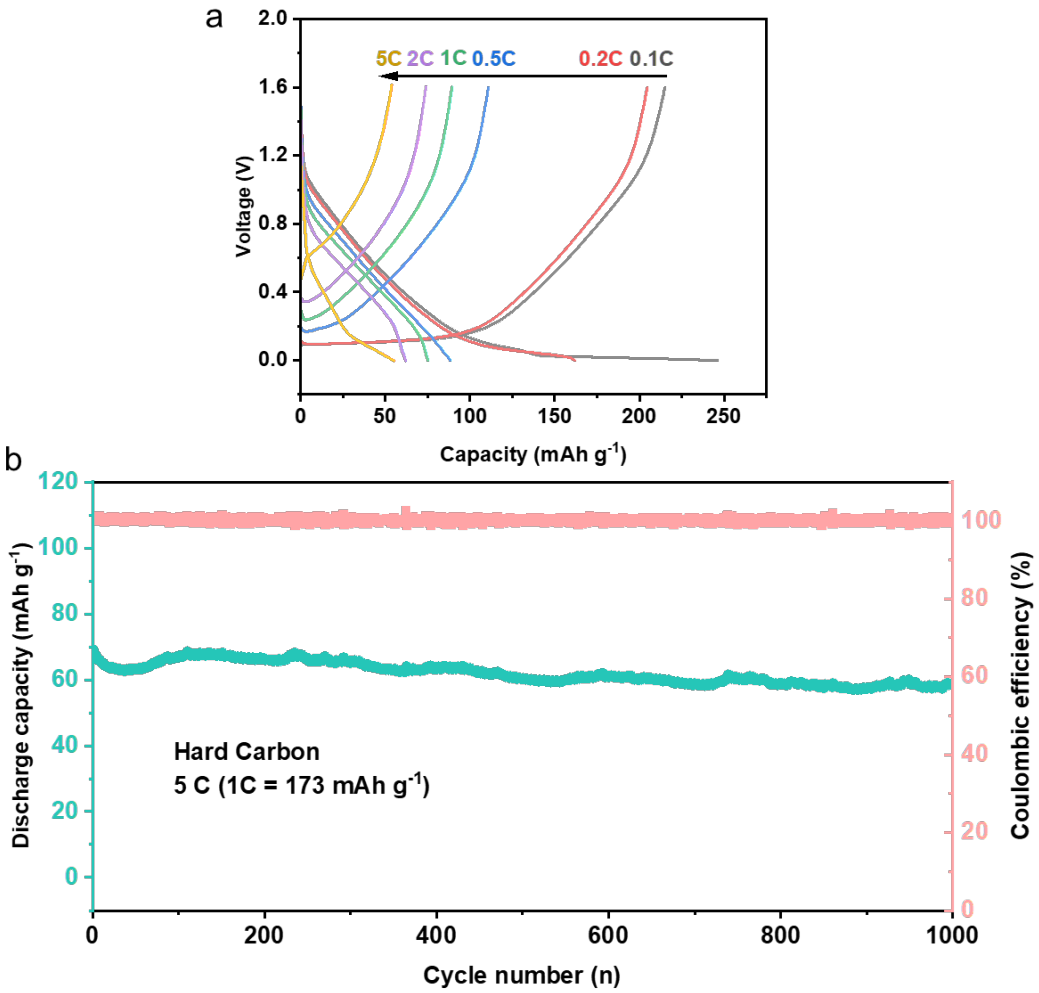

Figure S19. Performance of the hard carbon half cell**.** (a) Charge-discharge curves at different rate. (b) Cycle performance.

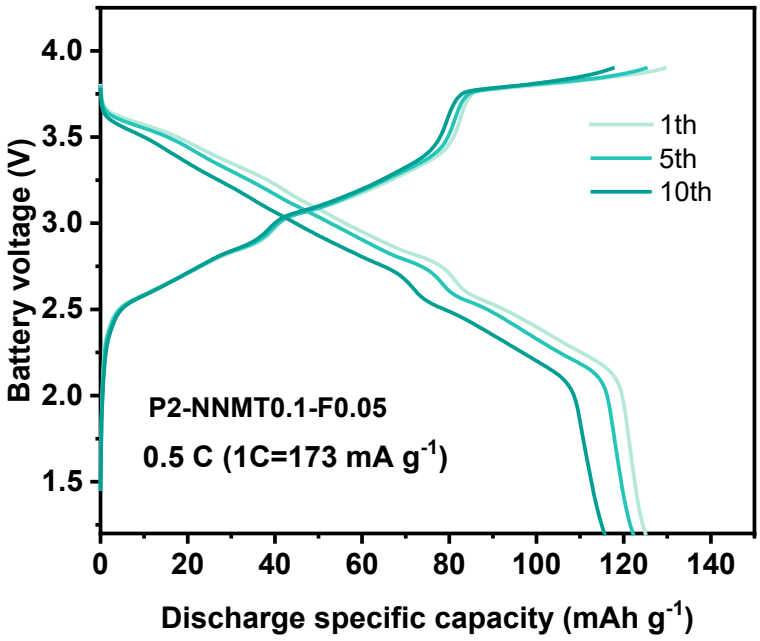

Figure S20. Charge-discharge curves of different cycling of the P2-NNMT0.5-F0.05//hard carbon full cell.

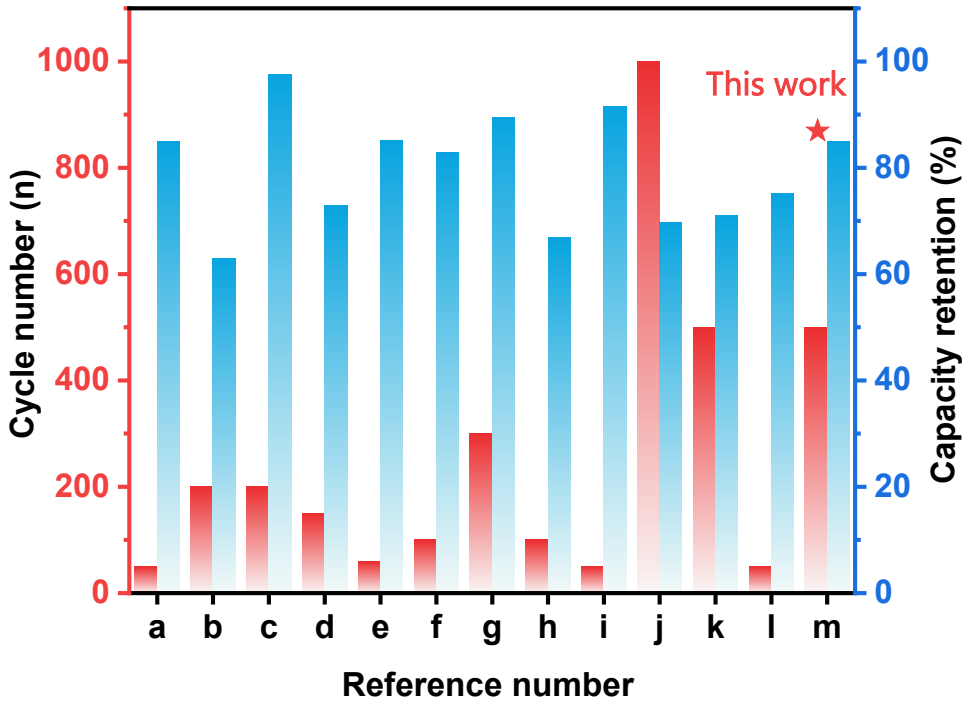

Figure S21. Comparison of the performance of Na-ion full cell ("a" to "m" are extracted sequentially from ref. [8–18]).

Table S1. ICP test results of NNM-Pristine and Ti and F co-doping sample

Chemical formula		Measured atomic ratio			
		Na	Ni	Mn	Ti
$Na_{0.67}Ni_{0.33}Mn_{0.67}O_2$	theoretically	0.67	0.33	0.67	
	actually	0.64	0.32	0.68	
$Na_{0.67}Ni_{0.33}Mn_{0.57}Ti_{0.1}O_{1.95}F_{0.05}$	theoretically	0.67	0.33	0.57	0.1
	actually	0.72	0.33	0.58	0.09

Table S2. Main parameters of processing and refinement

Compound	P2-NNM
Space group	P 63/m m c
a, Å	2.88965(8)
b, Å	2.88965(8)
c, Å	11.1610(8)
alpha	90
beta	90
gamma	120
V, Å^3	80.710(8)
Rwp	0.09
Rp	0.06
Chi*2	4.03

Table S3. Fractional atomic coordinates and isotropic displacement parameters of P2-NNM-

	x	y	z	Biso
Na1	0.3333	0.6667	0.2500	0.01266
Na2	0.0000	0.0000	0.2500	0.01266
Ni	0.0000	0.0000	0.0000	0.01266
Mn	0.0000	0.0000	0.0000	0.01266
O	0.3333	0.6667	0.5938	0.01266

Table S4. Main parameters of processing and refinement

Compound	P2-NNMT0.1
Space group	P 63/mmc
a, Å	2.90309(6)
b, Å	2.90309(6)
c, Å	11.1413(5)
alpha	90
beta	90
gamma	120
V, Å^3	81.32(5)
Rwp	0.11
Rp	0.084
Chi*2	2.81

Table S5. Fractional atomic coordinates and isotropic displacement parameters of P2-NNMT0.1

	x	y	z	Biso
Na1	0.3333	0.6667	0.2500	0.00500
Na2	0.0000	0.0000	0.2500	0.00500
Ni	0.0000	0.0000	0.0000	0.00500
Mn	0.0000	0.0000	0.0000	0.00500
O	0.3333	0.6667	0.5938	0.00500
Ti	0.0000	0.0000	0.0000	0.00500

Table S6. Main parameters of processing and refinement

Compound	P2-NNMT0.5-F0.05
Space group	P 63/m m c
a, Å	2.92569(2)
b, Å	2.92569(2)
c, Å	11.2582(7)
alpha	90
beta	90
gamma	120
V, Å^3	83.45(6)
Rwp	0.10
Rp	0.08
Chi*2	2.84

Table S7. Fractional atomic coordinates and isotropic displacement parameters of NNMT0.5-F0.05

	x	y	z	Biso
Na1	0.3333	0.6667	0.2500	0.11333
Na2	0.0000	0.0000	0.2500	0.06208
Ni	0.0000	0.0000	0.0000	0.01300
Mn	0.0000	0.0000	0.0000	0.07717
O	0.3333	0.6667	0.5938	0.03202
Ti	0.0000	0.0000	0.0000	0.05000
F	0.3333	0.6667	0.5938	0.05000

Table S8. Atomic in XPS at different etching depth of NNM-pristine samples

NNM-Pristine	Na 1s Atomic (%)	Ni 2p Atomic (%)	Mn 2p Atomic (%)	O1s Atomic (%)	C1s Atomic (%)
Not etching	17.50	7.07	12.09	51.36	11.97
Etching 7.5 nm	15.38	8.95	14.76	55.01	5.90
Etching 15 nm	13.19	10.12	17.03	54.82	4.83
Standard	18.25	9.26	18.25	54.4	/

Table S9. Atomic in XPS at different etching depth of 10% Ti doping and 5% F doping samples

10% Ti and 5% F doping	Na 1s Atomic (%)	Ni 2p Atomic (%)	Mn 2p Atomic (%)	O1s Atomic (%)	C1s Atomic (%)	Ti 2p Atomic (%)	F 1s Atomic (%)
Not etching	20.50	6.25	9.91	46.75	12.39	2.32	1.90
Etching 7.5 nm	19.94	7.97	12.49	47.45	7.67	2.63	1.86
Etching 15 nm	17.66	9.06	14.75	48.16	5.68	2.77	1.92
standard	18.13	9.20	15.3	53.45	/	2.7	1.3

Table S10. Cycling performance of layered oxide cathode in publications

Chemical formula	Voltage window (V)	Cycle performance	Reference
$Na_{2/3}Ni_{1/3}Mn_{2/3}O_2$	1.5–4.5	75.3% after 200 cycles at 2 C	[19]
$Na_{0.76}Ni_{0.20}Fe_{0.40}Mn_{0.40}O_2$	1.5–4.5	73.5% after 100 cycles at 0.1 C	[20]
P2-$Na_{0.55}[Ni_{0.1}Fe_{0.1}Mn_{0.8}]O_2$	1.5–4.3	80% after 500 cycles at 5 C	[21]
ZrO_2 coating $Na_{2/3}Ni_{1/3}Mn_{2/3}O_2$	2.0–4.5	77% after 200 cycles at 5 C	[22]
$Na_{2/3}Li_{1/6}Fe_{1/6}Co_{1/6}Ni_{1/6}Mn_{1/3}O_2$	2.0–4.5	63.7% after 300 cycles at 5 C	[23]
P2-type $Ni_{2/3}Ni_{1/4}Mg_{1/12}Mn_{2/3}O_2$	2.0–4.3	68.9% after 1000 cycles at 5 C	[9]
hierarchical $Na_{2/3}Ni_{1/3}Mn_{2/3}O_2$ hollow microspheres	2.5–4.2	83.3% after 500 cycles at 1 C	[16]
$Na_{2/3}Ni_{1/3}Mn_{2/3}O_{1.95}F_{0.05}$	2.0-4.0	75.6% after 2000 cycles at 10 C	[24]
$NaNi_{0.45}Cu_{0.05}Mn_{0.4}Ti_{0.1}O_2$	2.0-4.0	70.2% after 500 cycles at 1 C	[14]
$Na_{0.696}Ni_{0.329}Mn_{0.671}O_2$	2.5-4.13	71.9% after 1000 cycles at 1 C	[10]
P2-$Na_{0.7}Li_{0.03}Mg_{0.03}Ni_{0.27}Mn_{0.6}Ti_{0.07}O_2$	2.2–4.1	82% after 200 cycles at 2 C	[12]
P2-$Na_{0.67}Ni_{0.33}Mn_{0.57}T_{i0.1}O_{1.95}F_{0.05}$	2.3–4.3	80% after 500 cycles at 5 C	This work

Reference:

[1] B. H. Toby, R. B. Von Dreele, *J. Appl. Crystallogr.* **2013**, *46*, 544.

[2] B. Ravel, M. Newville, *J. Synchrotron Radiat.* **2005**, *12*, 537.

[3] A. M. Rappe, K. M. Rabe, E. Kaxiras, J. D. Joannopoulos, *Phys. Rev. B* **1990**, *41*, 1227.

[4] M. C. Payne, M. P. Teter, D. C. Allan, T. A. Arias, J. D. Joannopoulos, *Rev. Mod. Phys.* **1992**, *64*, 1045.

[5] S. J. Clark, M. D. Segall, C. J. Pickard, P. J. Hasnip, M. I. J. Probert, K. Refson, M. C. Payne, *Z. Für Krist. - Cryst. Mater.* **2005**, *220*, 567.

[6] H. J. Monkhorst, J. D. Pack, *Phys. Rev. B* **1976**, *13*, 5188.

[7] T. A. Halgren, W. N. Lipscomb, *Chem. Phys. Lett.* **1977**, *49*, 225.

[8] Y. Liu, Q. Shen, X. Zhao, J. Zhang, X. Liu, T. Wang, N. Zhang, L. Jiao, J. Chen, L.-Z. Fan, *Adv. Funct. Mater.* **2020**, *30*, 1907837.

[9] L. Zhang, C. Guan, Y. Xie, H. Li, A. Wang, S. Chang, J. Zheng, Y. Lai, Z. Zhang, *ACS Appl. Mater. Interfaces* **2022**, *14*, 18313.

[10] S. Liu, J. Wan, M. Ou, W. Zhang, M. Chang, F. Cheng, Y. Xu, S. Sun, C. Luo, K. Yang, C. Fang, J. Han, *Adv. Energy Mater.* **2023**, *13*, 2203521.

[11] Y. Li, S. Xu, X. Wu, J. Yu, Y. Wang, Y.-S. Hu, H. Li, L. Chen, X. Huang, *J. Mater. Chem. A* **2014**, *3*, 71.

[12] Z. Cheng, B. Zhao, Y.-J. Guo, L. Yu, B. Yuan, W. Hua, Y.-X. Yin, S. Xu, B. Xiao, X. Han, P.-F. Wang, Y.-G. Guo, *Adv. Energy Mater.* **2022**, *12*, 2103461.

[13] M.-Y. Shen, J.-S. Wang, Z. Ren, T. Wu, X. Liu, L. Chen, W.-C. Li, A.-H. Lu, *Adv. Funct. Mater.* **n.d.**, *n/a*, 2303812.

[14] K. Liu, S. Tan, J. Moon, C. J. Jafta, C. Li, T. Kobayashi, H. Lyu, C. A. Bridges, S. Men, W. Guo, Y. Sun, J. Zhang, M. P. Paranthaman, X.-G. Sun, S. Dai, *Adv. Energy Mater.* **2020**, *10*, 2000135.

[15] Y.-F. Zhu, Y. Xiao, S.-X. Dou, S.-L. Chou, *Cell Rep. Phys. Sci.* **2021**, *2*, 100631.

[16] J. Liang, Z. Li, J. Cheng, J. Qin, H. Liu, D. Wang, *Nano Res.* **2023**, *16*, 4987.

[17] Y.-N. Zhou, Z. Xiao, D. Han, S. Wang, J. Chen, W. Tang, M. Yang, L. Shao, C. Shu, W. Hua, D. Zhou, Y. Wu, *J. Mater. Chem. A* **2023**, *11*, 2618.

[18] R. Dong, F. Wu, Y. Bai, Q. Li, X. Yu, Y. Li, Q. Ni, C. Wu, *Energy Mater. Adv.* **2022**, *2022*, 9896218.

[19] X. Xia, T. Liu, C. Cheng, H. Li, T. Yan, H. Hu, Y. Shen, H. Ju, T. Chan, Z. Wu, Y. Su, Y. Zhao, D. Cao, L. Zhang, *Adv. Mater.* **2023**, *35*, 2209556.

[20] A. K. Paidi, W. B. Park, P. Ramakrishnan, S.-H. Lee, J.-W. Lee, K.-S. Lee, H. Ahn, T. Liu, J. Gim, M. Avdeev, M. Pyo, J. I. Sohn, K. Amine, K.-S. Sohn, T. J. Shin, D. Ahn, J. Lu, *Adv. Mater.* **2022**, *34*, 2202137.

[21] J.-Y. Hwang, J. Kim, T.-Y. Yu, Y.-K. Sun, *Adv. Energy Mater.* **2019**, *9*, 1803346.

[22] H. Ren, L. Zheng, Y. Li, Q. Ni, J. Qian, Y. Li, Q. Li, M. Liu, Y. Bai, S. Weng, X. Wang, F. Wu, C. Wu, *Nano Energy* **2022**, *103*, 107765.

[23] L. Yao, P. Zou, C. Wang, J. Jiang, L. Ma, S. Tan, K. A. Beyer, F. Xu, E. Hu, H. L. Xin, *Adv. Energy Mater.* **2022**, *12*, 2201989.

[24] Q. Liu, Z. Hu, M. Chen, C. Zou, H. Jin, S. Wang, Q. Gu, S. Chou, *J. Mater. Chem. A* **2019**, *7*, 9215.